

# An *Fgfr3-iCreER<sup>T2</sup>* Transgenic Mouse Line for Studies of Neural Stem Cells and Astrocytes

KAYLENE M. YOUNG, TOMOYUKI MITSUMORI, NIGEL PRINGLE, MATTHEW GRIST, NICOLETTA KESSARIS, AND WILLIAM D. RICHARDSON\*

The Wolfson Institute for Biomedical Research, University College London, London, United Kingdom

## KEY WORDS

*Fgfr3*; Cre-lox; transgenic mice; astrocytes; radial glia; neural stem cells; spinal cord; SVZ; olfactory bulb; interneurons

## ABSTRACT

The lack of markers for astrocytes, particularly gray matter astrocytes, significantly hinders research into their development and physiological properties. We previously reported that *fibroblast growth factor receptor 3* (*Fgfr3*) is expressed by radial precursors in the ventricular zone of the embryonic neural tube and subsequently by differentiated astrocytes in gray and white matter. Here, we describe an *Fgfr3-iCreER<sup>T2</sup>* phage artificial chromosome transgenic mouse line that allows efficient tamoxifen-induced Cre recombination in *Fgfr3*-expressing cells, including radial glial cells in the embryonic neural tube and both fibrous and protoplasmic astrocytes in the mature central nervous system. This mouse strain will therefore be useful for studies of normal astrocyte biology and their responses to CNS injury or disease. In addition, *Fgfr3-iCreER<sup>T2</sup>* drives Cre recombination in all neurosphere-forming stem cells in the adult spinal cord and at least 90% of those in the adult forebrain subventricular zone. We made use of this to show that there is continuous accumulation of all major interneuron subtypes in the olfactory bulb (OB) from postnatal day 50 (P50) until at least P230 (~8 months of age). It therefore seems likely that adult-born interneurons integrate into existing circuitry and perform long-term functions in the adult OB. © 2010 Wiley-Liss, Inc.

## INTRODUCTION

Astrocytes are the most abundant cells in the adult mouse brain, yet the paucity of molecular markers with which to identify astrocytes *in situ* means that they remain relatively poorly characterized. Two broad classes of astrocyte are recognized—fibrous astrocytes, found mainly in white matter; and protoplasmic astrocytes in the gray matter. Within these broad groupings there might be functionally specialized subtypes, for region-specific gene expression differences have been reported (Hochstim et al., 2008). At least some astrocytes develop by direct trans-differentiation of radial glial cells after they have undergone their final divisions (Hirano and Goldman, 1988; Voigt, 1989). On the basis of the development of their densely ramified fine processes and exclusive territories (Bushong et al., 2004; Nagy and Rash, 2003), they are said to reach maturity

between postnatal day 17 (P17) and P30. Unlike the neuronal or oligodendroglial lineages, we have no simple way of distinguishing astrocytes at different stages of maturation, which impedes study of their differentiation and plasticity in the normal or injured brain.

Glial fibrillary acidic protein (GFAP) is expressed strongly by fibrous astrocytes in white matter and at the pial surface but is absent from the vast majority of gray matter (protoplasmic) astrocytes in the normal healthy CNS. Antibodies to S100 $\beta$  are often used to mark GFAP-negative protoplasmic astrocytes (Ludwin et al., 1976), but this protein is also expressed by some oligodendrocyte (OL) lineage cells (Hachem et al., 2005; Vives et al., 2003; Zuo et al., 2004). Therefore, identifying astrocytes unambiguously *in vivo* has proven difficult. We previously reported that the *fibroblast growth factor receptor 3* (*Fgfr3*) transcripts are expressed in the ependymal zone (EZ) of the embryonic spinal cord and subsequently become restricted to astrocytes in the gray and white matter of the postnatal cord (Pringle et al., 2003). *Fgfr3* has been used subsequently for *in situ* studies of astrocyte development (Agius et al., 2004; Hochstim et al., 2008).

*Fgfr3* is also expressed in the ventricular zone (VZ) of the developing brain (Bansal et al., 2003). A constitutive activating mutation of FGFR3 has also been associated with increased MAPK activity and increased proliferation of cells in the VZ (Inglis-Broadgate et al., 2005; Thomson et al., 2007). These data indicate that FGFR3 is expressed by neuroepithelial precursors and/or radial glial cells in the brain, as in the spinal cord. Many *Fgfr3*<sup>+</sup> cells in the postnatal brain are found outside the VZ (Bansal et al., 2003), similar to the spinal cord (Pringle et al., 2003). *Fgfr3* expression both *in vivo* and in cultured neural cells has been linked to OL lineage cells as well as astrocytes (Bansal et al., 2003; Miyake et al., 1996; Oh et al., 2003). However, *Fgfr3* is

Additional Supporting Information may be found in the online version of this article.

William D. Richardson and Nicoletta Kessariss contributed equally to this article.

Tomoyuki Mitsumori is currently at Department of Pharmacology, Kyoto University Graduate School of Medicine, Konoe-Cho Yoshida Sakyo-ku Kyoto 606-8315, Japan

Grant sponsors: MRC, The Wellcome Trust.

\*Correspondence to: William D. Richardson, The Wolfson Institute for Biomedical Research, University College London, Gower Street, London WC1E 6BT, United Kingdom. E-mail: w.richardson@ucl.ac.uk

Received 13 October 2009; Accepted 13 January 2010

DOI 10.1002/glia.20976

Published online 12 February 2010 in Wiley InterScience (www.interscience.wiley.com).

expressed at a low level in early oligodendrocyte precursors (OLPs) and is upregulated only transiently as they start to differentiate into OLs (Bansal et al., 1996), so it is to be expected that the great majority of *Fgfr3*<sup>+</sup> cells in the postnatal CNS should be astrocytes, not OL lineage cells. Consistent with this, Cahoy et al. (2008) immunopurified astrocytes from early postnatal brains (P1–P30) of *S100β-eGFP* mice and showed that *Fgfr3* mRNA was highly enriched relative to other purified neural cell types on Affymetrix gene microarrays.

Here, we describe the generation and characterization of a phage artificial chromosome (PAC) transgenic mouse line that expresses tamoxifen-inducible Cre (“codon-improved” version, *iCreER*<sup>T2</sup>) under *Fgfr3* transcriptional control. This has allowed us to identify and study *Fgfr3*<sup>+</sup> cells in the developing and/or adult CNS. We have confirmed that *Fgfr3* is expressed by radial glial stem cells in the embryonic brain and spinal cord and by fibrous and protoplasmic astrocytes in the postnatal CNS. In addition, we show that *Fgfr3* is expressed by adult neural stem cells located within the subventricular zone (SVZ) of the forebrain and the EZ of the spinal cord. We followed the development of olfactory bulb (OB) interneurons from SVZ stem cells during adulthood and showed that all identifiable interneuron subtypes accumulate and survive long term (>6 months) in the granule and periglomerular layers of the OB. We expect that our *Fgfr3-iCreER*<sup>T2</sup> line will be useful for further studies of OB neurogenesis and studies of astrocytes in the postnatal CNS. In addition, it is likely that the line will find uses for studies of non-CNS tissues that normally express *Fgfr3*, such as developing cartilage and bone.

## MATERIALS AND METHODS

### Transgenesis

The mouse genomic PAC library RPCI 21 from the UK Human Genome Mapping Project Resource Center was screened with a 900-bp PCR-generated fragment from a rat *Fgfr3* cDNA, corresponding to most of the extracellular domain. One positive clone (608P12) was selected for modification. It contained an ~180 kb insert, including 37 kb upstream and 130 kb downstream of the *Fgfr3* gene. The targeting construct was designed to insert an *iCreER*<sup>T2</sup>-*SV40polyA* cassette into exon 2 of the *Fgfr3* gene, fusing it to the endogenous initiation codon and deleting 58 bp immediately downstream. *iCreER*<sup>T2</sup> (Claxton et al., 2008) is a fusion between *iCre* (excluding the nuclear localization signal) (Shimshek et al., 2002) and the ER<sup>T2</sup> component of CreER<sup>T2</sup> (Indra et al., 1999). PAC recombination and screening were as described (Lee et al., 2001; Rivers et al., 2008). The modified PAC was digested with Sgf1, which recognizes a single site in the PAC vector backbone. The linear PAC was purified by pulsed field gel electrophoresis, and transgenic mice were generated by pronuclear injection. Five founders were identified by Southern blotting. Three produced fertile transgenic offspring, which gave indistinguishable Cre mRNA expression patterns. All data here refer to

founder #4-2, which can be requested online at <http://www.ucl.ac.uk/~ucbwdr/Richardson.htm>.

### Genotyping and Embryo Staging

All animal work conformed to the Animals (Scientific Procedures) Act 1986 and was approved by the UK Government Home Office. Genotyping was performed by PCR using primers *iCre250* (GAG GGA CTA CCT CCT GTA CC) and *iCre880* (TGC CCA GAG TCA TCC TTG GC) which amplify a 630-bp fragment. The amplification program was: 94°C/4 min, followed by 33 cycles of 94°C/30 s, 61°C/45 s, 72°C/1 min and finally 72°C/10 min. Heterozygous *Fgfr3-iCreER*<sup>T2</sup> mice were crossed to *R26R-GFP* (Mao et al., 2001), *R26R-YFP* (Srinivas et al., 2001), or *Z/EG* (Novak et al., 2000) Cre-conditional reporters and double-heterozygous offspring selected for analysis. *R26R-GFP* and *R26R-YFP* transgenes were identified by PCR of tail DNA as described (Psachoulia et al., in press). The *Z/EG* transgene was identified by whole mount β-galactosidase labeling of tail tissue.

For timed matings, breeders were caged together overnight and vaginal plugs scored the following morning. Midday of the day of the vaginal plug was designated embryonic day 0.5 (E0.5). Pregnant females were killed by CO<sub>2</sub> inhalation and the embryos removed. Embryonic ages were confirmed by morphological criteria (Theiler, 1972).

### Tamoxifen Administration

Tamoxifen was dissolved in corn oil at 40 mg/mL and administered by oral gavage. Adult mice (P50 or older) received 200 mg/kg body weight once a day for 5 days. Pregnant females received a single dose of 200 mg/kg body weight. Time after tamoxifen administration is denoted as e.g. P50 + 7, where +7 refers to the number of days after the *first* dose given on P50.

### BrdU Administration

BrdU (Sigma) was dissolved in phosphate buffered saline (PBS) at 20 mg/mL, and 50 μL was administered intra-peritoneally to adult mice four times in 24 h (6 a.m., noon, 6 p.m., midnight).

### Tissue Preparation and Immunohistochemistry

Tissue fixation, and immunohistochemistry employed methods and antibodies as described previously (Rivers et al., 2008; Young et al., 2007). Additional antibodies were as follows: rabbit anti-Aquaporin-4 (Chemicon; 1:500); guinea-pig anti-GLAST (Chemicon; 1:5,000); mouse anti-RC2 monoclonal IgM supernatant (Developmental Studies Hybridoma Bank; 1:4). Sections of adult tissue (30 μm) were immunolabeled as floating sections

and transferred to glass slides for mounting and microscopy. Embryonic brain and spinal cord sections were collected directly onto coated glass slides.

### ***In Situ* Hybridization**

Sections (20  $\mu$ m) for *in situ* hybridization were collected on the surface of DEPC-treated PBS, transferred onto glass slides and allowed to dry in air at 20–25°C. The *Fgfr3* RNA hybridization probe has been described (Pringle et al., 2003). For the *iCreER<sup>T2</sup>* probe, *iCreER<sup>T2</sup>* coding sequences were PCR amplified using primers that added a 5' SalI site and a 3' EcoRI site. The PCR product was cloned into pBluescript along with a 3' SV40-*polyA* sequence. The antisense probe was transcribed with T3 RNA polymerase (Promega) from SalI-linearized template in the presence of digoxigenin- or fluorescein-conjugated nucleotide mix (Roche). For details see <http://www.ucl.ac.uk/~ucbzwdr/Richardson.htm>.

### **Neurosphere Cultures**

Primary neurosphere cultures were generated from the entire spinal cord or the micro-dissected SVZ of tamoxifen-treated *Fgfr3-iCreER<sup>T2</sup>:R26R-YFP* mice at P70 + 7, P70 + 14, P70 + 21, and P70 + 56. At each time, separate cultures were established from three individual mice. Tissue was chopped into small pieces, digested with Trypsin-EDTA (Invitrogen) at 37°C for 12 min and digestion stopped with soybean trypsin inhibitor (Sigma). Single-cell suspensions were produced by trituration in calcium- and magnesium-free Earles Buffered Salt Solution (Invitrogen). Dissociated cells from each mouse were plated in one (SVZ) or two (spinal cord) six-well tissue culture plates in Neurocult basal medium for neural stem cells with Neurocult neural stem cell proliferation supplement (9:1, Stem Cell Technologies), plus 10 ng/mL basic fibroblast growth factor (Roche), 20 ng/mL epidermal growth factor (Sigma), and 4  $\mu$ g/mL heparin (sodium salt, Sigma). Cultures were maintained at 37°C in a 5% (v/v) CO<sub>2</sub> atmosphere. Half of the spinal cord culture medium was replaced at 7 days. The fractions of YFP<sup>+</sup> neurospheres were determined by fluorescence microscopy at 7 days (SVZ) or 14 days (spinal cord).

### **Microscopy and Data Analysis**

Confocal images were collected as single scans (1  $\mu$ m) using an Ultraview confocal microscope (Perkin Elmer). For quantification, a series of nonoverlapping images (20 $\times$  objective lens) were collected from selected adult brain regions (at least 8 micrographs/region/section). Three brain sections from each of three mice were counted for each staining condition (at least 300 labeled cells in total). The brain regions analyzed are illustrated in Supporting Information Figure 1. Statistical compar-

isons were made by *t*-test or, for multiple regions or time points, by ANOVA. Differences were considered to be statistically significant at  $P < 0.05$ .

## **RESULTS**

### ***Fgfr3* as a Marker for Cortical Astrocytes**

Following from our previous study of mouse spinal cord (Pringle et al., 2003), we examined *Fgfr3* as a candidate marker for astrocytes in the postnatal brain. By *in situ* hybridization we detected many *Fgfr3*<sup>+</sup> cells in the adult mouse cerebral cortex (Fig. 1). These cells did not co-express NG2, OLIG2, or NeuN (Fig. 1a–c), indicating that they were not OL lineage cells or neurons. The majority of *Fgfr3*<sup>+</sup> cells were GFAP-negative but all GFAP<sup>+</sup> cells co-expressed *Fgfr3* (Fig. 1d). Since most cortical astrocytes do not express GFAP, this was consistent with the notion that *Fgfr3* is expressed by astrocytes in the adult mouse cortex.

### **Expression of an *Fgfr3-iCreER<sup>T2</sup>* PAC Transgene in the CNS**

To characterize the *Fgfr3*<sup>+</sup> cells further, we generated transgenic mouse lines that express *iCreER<sup>T2</sup>* under the transcriptional control of *Fgfr3* in a PAC (Fig. 1e and Methods). We obtained five founders, three of which transmitted the *Fgfr3-iCreER<sup>T2</sup>* transgene to their offspring. We characterized each founder by *in situ* hybridization for *Fgfr3* and *iCreER<sup>T2</sup>* on adjacent sections of embryonic spinal cords. *Fgfr3* and *iCreER<sup>T2</sup>* had similar expression patterns at all ages examined (Supp. Info. Fig. 2). At the earliest times (embryonic day 11.5, E11.5), expression was restricted to cell bodies in the EZ. We identified these EZ cells as pluripotent radial precursors that generate neurons, astrocytes, and OLs during embryonic development (Supp. Info. Fig. 2). Subsequently, *Fgfr3*- and *iCreER<sup>T2</sup>*-positive cells moved away from the EZ into the developing gray and white matter, where they persisted long term (Supp. Info. Fig. 2).

In the postnatal spinal cord and brain, there were many *Fgfr3*<sup>+</sup> cells in gray and white matter (Fig. 1 and Supp. Info. Fig. 2). In adult *Fgfr3-iCreER<sup>T2</sup>* mice, these *Fgfr3*<sup>+</sup> cells co-expressed *iCreER<sup>T2</sup>* (Fig. 1f). We tentatively concluded that expression of the *Fgfr3-iCreER<sup>T2</sup>* transgene mimics normal *Fgfr3* expression in the embryonic and adult spinal cord and adult forebrain.

### ***Fgfr3-iCreER<sup>T2</sup>* Marks Protoplasmic and Fibrous Astrocytes**

*Fgfr3-iCreER<sup>T2</sup>* was crossed into the *Rosa26R-YFP* (*R26R-YFP*) background (Srinivas et al., 2001), tamoxifen was administered from P50 and the mice analyzed subsequently by immunolabeling for YFP (see Methods). On P50 + 5, no YFP-labeled cells were detected

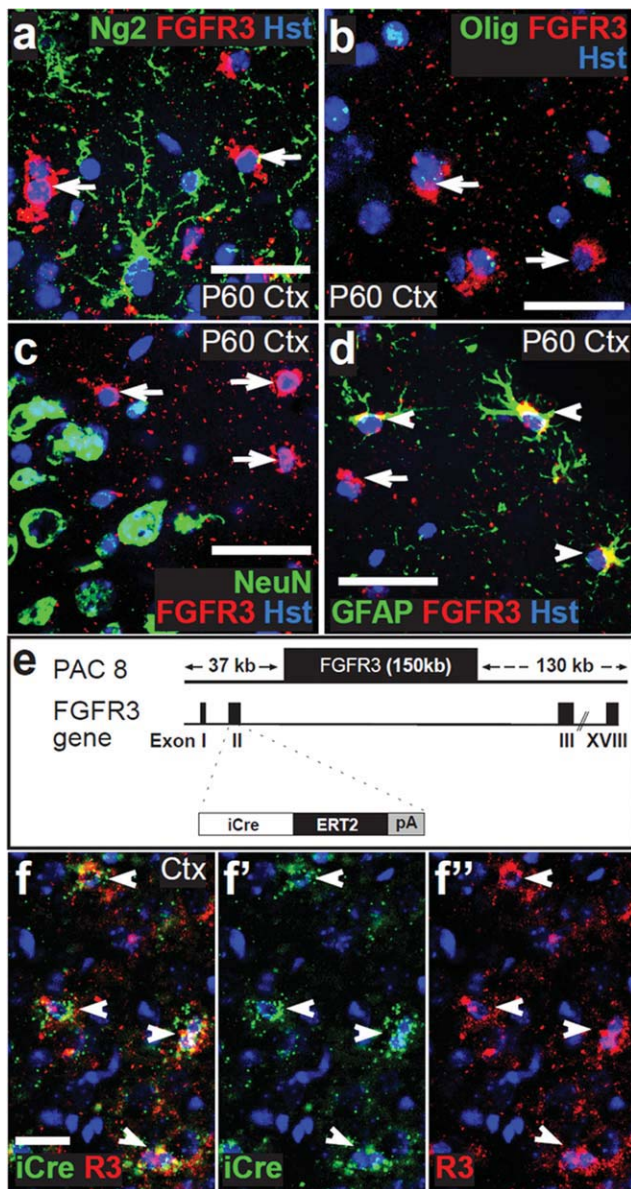


**Fig. 1.** *Fgfr3* mRNA in astrocytes of the adult mouse cerebral cortex. Cells expressing *Fgfr3* transcripts were distributed throughout all regions of the P60 forebrain. In single confocal scans (1  $\mu$ m) from the medial cortex *Fgfr3*<sup>+</sup> cells were negative for NG2 (a), OLIG2 (b), or NeuN (c). GFAP-positive cells co-expressed *Fgfr3* (d). A PAC containing ~37 kb upstream and 110 kb downstream of the mouse *Fgfr3* locus was modified by insertion of *iCreER*<sup>T2</sup> into exon 2 immediately downstream of the endogenous initiation codon (e). (f) Double-fluorescence *in situ* hybridization confirmed that *Fgfr3* (R3, red) and *iCreER*<sup>T2</sup> (*iCre*, green) are expressed within the same cells (arrowheads) in the medial cortex of P60 *Fgfr3-iCreER*<sup>T2</sup> mice (single 1  $\mu$ m scan). Sections were counterstained with Hoechst 33258 (Hst, blue) to visualize cell nuclei. Single-labeled (arrows) and double-labeled cells (arrowheads) are indicated. Scale bars: 25  $\mu$ m.

anywhere in the CNS, either because recombination had not yet occurred or because the level of YFP protein was still below detectable levels. However, at P50 + 7 many YFP<sup>+</sup> cells were found throughout the gray matter of the brain (Fig. 2) and spinal cord (Supp. Info. Fig. 2). These cells were close-packed and filled almost the

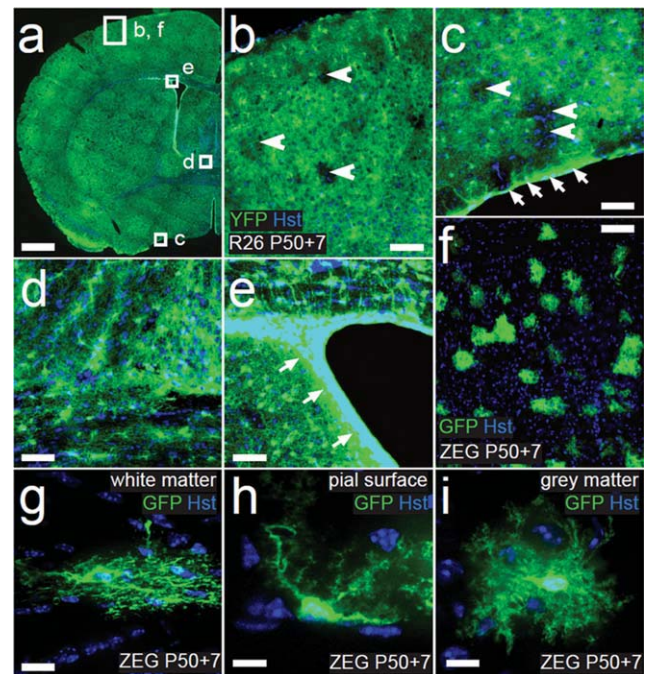


**Fig. 2.** Tamoxifen administration to *Fgfr3-iCreER*<sup>T2</sup> transgenic mice. YFP immunolabeling of 30  $\mu$ m coronal forebrain sections of P50 + 7 *Fgfr3-iCreER*<sup>T2</sup>:*R26R-YFP* mice (a–e). Arrows in (c) and (e) (higher-magnification images of the indicated regions in (a)) reveal intense YFP labeling under the pial surface and in the SVZ of the lateral ventricle, respectively. Reporter gene activation was very efficient and YFP-labeled cells were widespread and ubiquitous in the gray and white matter (b, d). To visualize the morphology of individual cells, we switched to the *Z/EG* reporter (f–i), in which recombination was less efficient than *R26-YFP* (compare b and f), so that labeled cells could be seen in isolation (g–i). At P50 + 7, the morphologies of GFP<sup>+</sup> cells resembled fibrous white matter astrocytes (g), sub-pial astrocytes (h), and protoplasmic astrocytes (i). Sections were counterstained with Hoechst 33258 (Hst) to visualize cell nuclei. Scale bars: 0.8 mm (a), 40  $\mu$ m (b–f), or 8  $\mu$ m (g–i).

entire gray matter volume with YFP fluorescence. Within this sea of fluorescence were scattered “holes,” corresponding to unlabeled cells (e.g. Fig. 2a–c, arrowheads). This pattern was consistent with the idea that the YFP-labeled cells were astrocytes and indicated that the efficiency of *R26R-YFP* reporter gene activation was high, though less than 100%. We never observed any YFP<sup>+</sup> cells in *Fgfr3-iCreER*<sup>T2</sup>:*R26R-YFP* mice that had not received tamoxifen.

The great majority of YFP<sup>+</sup> cells in *R26R-YFP* reporters were S100 $\beta$ <sup>+</sup> (94%  $\pm$  4% of YFP<sup>+</sup> cells) and most of these were GFAP-negative (Fig. 3a–c,m). This fits the idea that the YFP<sup>+</sup> cells are protoplasmic astrocytes, which normally express low or undetectable levels of GFAP. The minority of cortical YFP<sup>+</sup> cells that was GFAP<sup>+</sup> (18%  $\pm$  4%) tended to be associated with blood vessels or the pial surface (Fig. 3d). Those that contacted blood vessels frequently also expressed Aquaporin-4 (Fig. 3e). A very small number of YFP<sup>+</sup> cortical cells co-expressed the neuronal marker NeuN (0.2%  $\pm$  0.4% of YFP<sup>+</sup> cells) or the OL lineage marker OLIG2 (1.0%  $\pm$  0.6% of YFP<sup>+</sup> cells) (Fig. 3f–i,m). These double-labeled cells did not localize to any particular region of

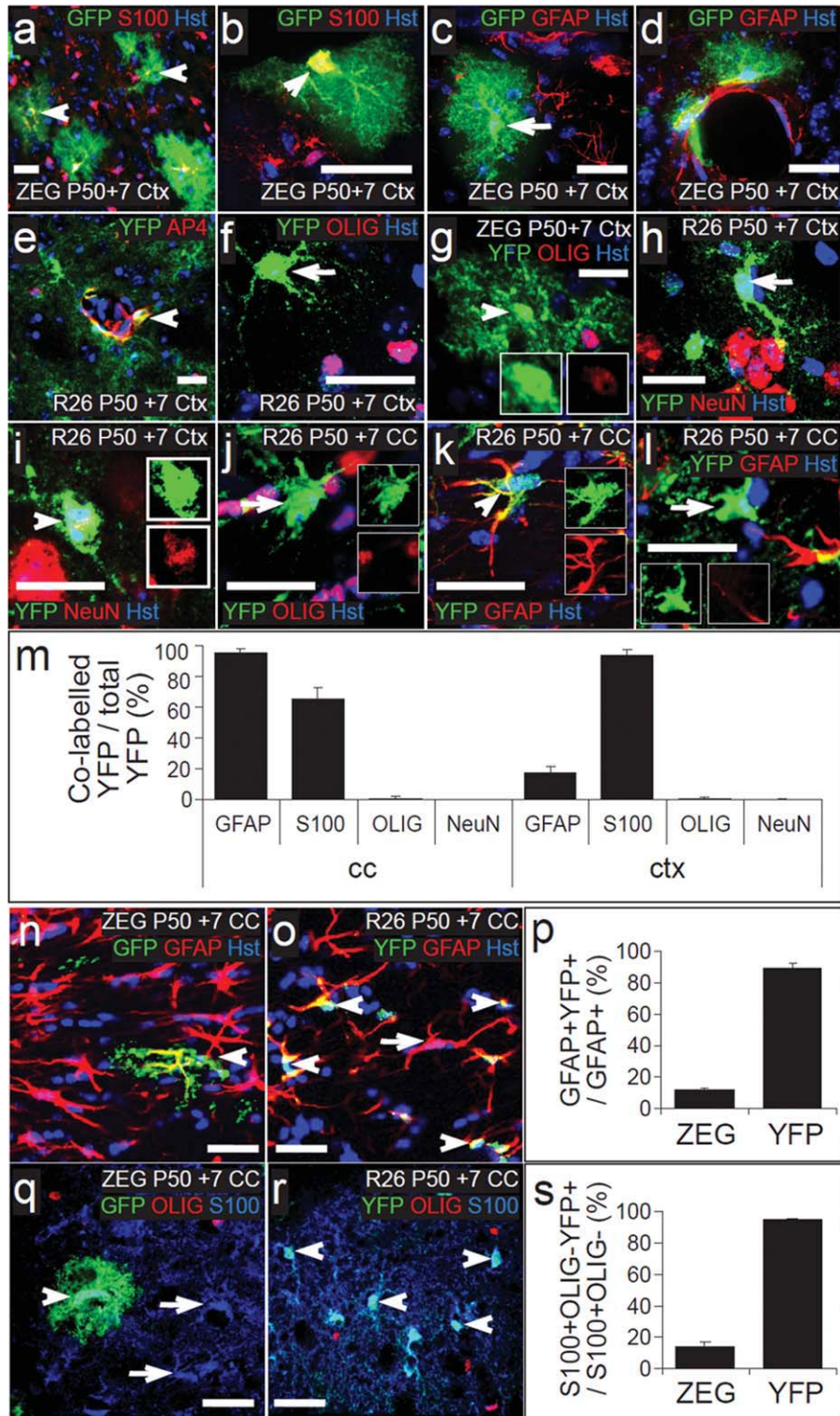


Fig. 3. *Fgfr3-CreER<sup>T2</sup>* marks astrocytes in the adult mouse fore-brain. To determine the identity of *Fgfr3*<sup>+</sup> cells, 30  $\mu$ m coronal fore-brain sections of P50 + 7 *Fgfr3-iCreER<sup>T2</sup>:Z/EG* (a-d, g, n, q) or *Fgfr3-iCreER<sup>T2</sup>:R26R-YFP* mice (e, f, h-l, o, r) were co-immunolabeled for GFP or YFP, respectively, and neural cell type-specific markers. The vast majority of GFP/YFP<sup>+</sup> cells in the medial cortex co-labeled for S100 $\beta$  (a, b), but not GFAP (c). However, GFP/YFP<sup>+</sup> cells co-labeled for GFAP (d) and Aquaporin-4 (AP4) (e) when they were associated with blood vessels. GFP/YFP<sup>+</sup> cells were mostly negative for OLIG2 (f) or NeuN (h), although there were rare exceptions (g, i). In the corpus callosum, the great majority of GFP/YFP<sup>+</sup> cells were OLIG2-negative (j) but GFAP<sup>+</sup> (k, n, o). Occasional cells that were GFAP-negative were observed (l). The proportions of YFP<sup>+</sup> cells in the corpus callosum and

medial cortex of *Fgfr3-iCreER<sup>T2</sup>:R26R-YFP* mice that co-express GFAP, S100 $\beta$ , OLIG2 or NeuN were quantified (m). Not all GFAP<sup>+</sup> fibrous astrocytes were GFP/YFP<sup>+</sup> in the corpus callosum of P50 + 7 *Fgfr3-iCreER<sup>T2</sup>:Z/EG* (n) or *Fgfr3-iCreER<sup>T2</sup>:R26R-YFP* (o). Not all S100 $\beta$ <sup>+</sup>, OLIG2-negative protoplasmic astrocytes were GFP/YFP<sup>+</sup> in the cortex of P50 + 7 *Fgfr3-iCreER<sup>T2</sup>:Z/EG* (q) or *Fgfr3-iCreER<sup>T2</sup>:R26R-YFP* (r). Reporter-specific recombination efficiencies (fractions of fibrous or protoplasmic astrocytes that were GFP/YFP<sup>+</sup>) are shown (p, s). Sections were counterstained with Hoechst 33258 (Hst) to visualize cell nuclei. Images are single confocal scans (1  $\mu$ m). Examples of single-positive (arrows) and double-immuno-positive cells (arrowheads) are indicated. Ctx, cortex; CC, corpus callosum. Scale bars: 25  $\mu$ m (a-e, n, o, q, r), 15  $\mu$ m (f-l).

the forebrain. Many (around half) of the OLIG2<sup>+</sup>, YFP<sup>+</sup> cells expressed a low level of OLIG2 relative to the OLIG2<sup>+</sup>, YFP-negative cells (Fig. 3g). Although S100 $\beta$  is widely used to detect protoplasmic astrocytes, it is also expressed by some OL lineage cells (Hachem et al., 2005; Vives et al., 2003). We therefore triple-labeled for YFP, S100 $\beta$ , and OLIG2. The great majority (92%  $\pm$  5%) of YFP<sup>+</sup> cells co-expressed S100 $\beta$  but not OLIG2 (Fig. 3r), confirming them as astrocytes.

In coronal sections of P50 + 7 corpus callosum, a major white matter tract, the vast majority (95%  $\pm$  3%) of YFP<sup>+</sup> cells were GFAP<sup>+</sup> fibrous astrocytes (Fig. 3k-m, o). A very small proportion (1.0%  $\pm$  0.8%) of YFP<sup>+</sup> cells co-labeled for OLIG2 (Fig. 3j, m) but none co-labeled for NeuN (Fig. 3m). A tiny minority of all SOX10<sup>+</sup> OL lineage cells (0.07%  $\pm$  0.01%) co-expressed YFP<sup>+</sup>. Similarly, a tiny fraction of NG2<sup>+</sup> OL precursors (0.3%  $\pm$  0.1%) were YFP<sup>+</sup>. Taken together, these data demonstrate that recombination in the *R26R-YFP* reporter background is both efficient and astrocyte-specific.

To examine the detailed morphology of labeled cells we used the *Z/EG* reporter, in which eGFP is expressed in a Cre-inducible manner from a synthetic promoter composed of CMV and  $\beta$ -actin promoter elements (Novak et al., 2000). *Z/EG* reporters recombined less efficiently (fewer cells labeled) than *R26R-YFP* (compare Fig. 2b and Fig. 2f). In P50 + 7 corpus callosum only 12%  $\pm$  1% of GFAP<sup>+</sup> astrocytes were GFP<sup>+</sup> in the *Z/EG* reporter (Fig. 3n, p), compared with 89%  $\pm$  4% in *R26R-YFP* reporters. In the cortex, 14%  $\pm$  4% of S100 $\beta$ <sup>+</sup>, OLIG2-negative protoplasmic astrocytes were GFP<sup>+</sup> in *Z/EG* reporters, compared with 95%  $\pm$  1% in *R26R-YFP* (Fig. 3q-s). Nevertheless, expression of GFP in individual, isolated cells was very high in *Z/EG* reporters so that even fine processes were visible by GFP immunolabeling. The morphologies of GFP<sup>+</sup> cells in the corpus callosum (Fig. 2g) and at the pial surface (Fig. 2h) resembled fibrous white matter astrocytes and subpial astrocytes, respectively. In the cortical gray matter, GFP<sup>+</sup> cells had a dense halo of very fine processes around their cell bodies, giving them the distinct “bushy” or “fuzzy” morphology typical of protoplasmic astrocytes (Fig. 2i).

### Long-Term Stability of *Fgfr3*-Expressing Astrocytes in the Cortex

To investigate the long-term fates of *Fgfr3*-expressing cells in the adult CNS, we immunolabeled coronal forebrain sections of P50 + 14 and/or P50 + 80 *Fgfr3-iCreER<sup>T2</sup>:R26R-YFP* mice for YFP and either GFAP (to identify fibrous astrocytes) or with S100 $\beta$  and OLIG2 (to identify S100 $\beta$ <sup>+</sup>, OLIG2-negative protoplasmic astrocytes) (Fig. 4).

In the cortex between P50 + 7 and P50 + 80, there was no significant change in the proportion of YFP<sup>+</sup> protoplasmic astrocytes (92%  $\pm$  5% vs. 97%  $\pm$  1%, respectively) nor was there a change in the proportion of

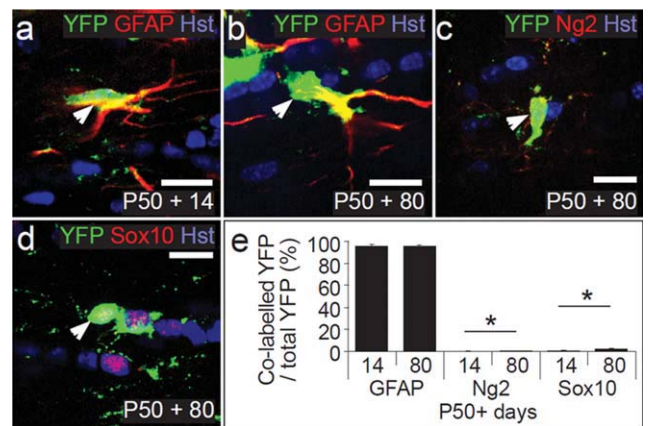


Fig. 4. Lineage tracing of astrocytes in the corpus callosum. 30  $\mu$ m coronal sections of P50 + 14 and P50 + 80 *Fgfr3-iCreER<sup>T2</sup>:R26R-YFP* mouse forebrain were immunolabeled for YFP and neural cell type-specific markers. At both P50 + 14 (a) and P50 + 80 (b) almost all YFP<sup>+</sup> cells (green) in the corpus callosum were GFAP<sup>+</sup> fibrous astrocytes (red). A small fraction of YFP<sup>+</sup> cells co-labeled for NG2 (c) or SOX10 (d). These data were quantified (e). Images are single confocal scans (1  $\mu$ m). Sections were counterstained with Hoechst 33258 (Hst) to visualize cell nuclei. Single asterisk indicates  $P < 0.05$ . Scale bar: 10  $\mu$ m.

YFP<sup>+</sup> cells that labeled for OLIG2 (1.0%  $\pm$  0.6% vs. 1.0%  $\pm$  1.0%) or NeuN (0.2%  $\pm$  0.4% vs. 0.3%  $\pm$  0.3%).

In the corpus callosum, there was no significant change in the proportion of YFP<sup>+</sup> cells that were GFAP<sup>+</sup> fibrous astrocytes (>95% at all ages from P50 + 7 to P50 + 80) (Fig. 4a, b, e). However, we found a small but significant accumulation of YFP<sup>+</sup> oligodendroglial cells with time (Fig. 4c-e). Between P50 + 14 and P50 + 80 the proportion of YFP<sup>+</sup> cells that was NG2<sup>+</sup> increased ~3-fold from ~0.2% to ~0.6%, and the proportion of YFP<sup>+</sup> cells that was SOX10<sup>+</sup> increased from ~0.8% to ~2.3% (significance,  $P < 0.01$ ; Fig. 4e). These presumptive OL lineage cells might be derived from *Fgfr3*<sup>+</sup> astrocytes. However, a small number of OLs in the adult corpus callosum is generated throughout life by SVZ stem cells (Menn et al., 2006; Rivers et al., 2008). Therefore, it seemed possible that in addition to labelling astrocytes our *Fgfr3-iCreER<sup>T2</sup>* transgene might target SVZ stem cells.

### *Fgfr3*<sup>+</sup> Neural Stem Cells in the Spinal Cord EZ and Forebrain SVZ

We previously noted that the spinal cord EZ was YFP-labeled in embryonic *Fgfr3-iCreER<sup>T2</sup>:R26R-YFP* mice. This EZ labeling also persisted in the adult spinal cord (Supp. Info. Fig. 2). In addition, the forebrain SVZ was heavily YFP-labeled (Fig. 2e, arrows). This suggested that *Fgfr3-iCreER<sup>T2</sup>* might induce recombination in neural stem cells, which are present in both the EZ and the SVZ (Doetsch et al., 1999; Hamilton et al., 2009; Weiss et al., 1996). Consistent with this, some YFP<sup>+</sup> cells in the SVZ co-expressed GFAP, which marks SVZ stem cells (“subependymal astrocytes” or “type-B cells”) (Doetsch et al., 1999; Laywell et al., 2000) (Fig. 5a).

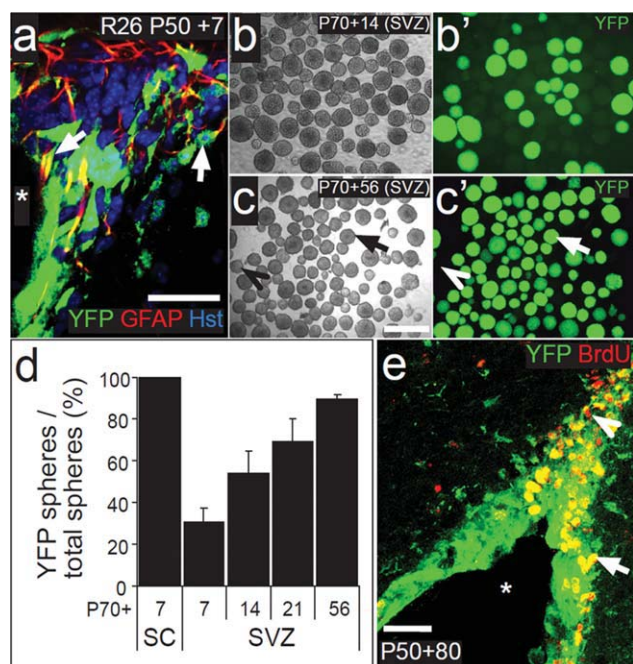


**Fig. 5.** *Fgfr3-CreER<sup>T2</sup>* marks neurosphere-forming cells in the SVZ. (a) Many YFP<sup>+</sup> cells in the SVZ of *Fgfr3-iCreER<sup>T2</sup>:R26R-YFP* mice at P50 + 7 are GFAP<sup>+</sup> (single confocal scan; lateral ventricle indicated by an asterisk). Neurosphere cultures were generated from the spinal cord (SC) and forebrain SVZ of *Fgfr3-iCreER<sup>T2</sup>:R26R-YFP* mice at P70 + 7, P70 + 14 (b phase; b' fluorescence), P70 + 21 and P70 + 56 (c, phase; c', fluorescence). A YFP<sup>+</sup> neurosphere (arrow) and a YFP-negative neurosphere (arrowhead) are indicated. The proportion of neurospheres that was YFP<sup>+</sup> was determined for each chase period (d). 100% of SC neurosphere-forming cells were YFP<sup>+</sup> within 7 days of tamoxifen administration (P70 + 7), and the fraction of YFP<sup>+</sup> SVZ-derived neurospheres increased with time to ~90%. BrdU was administered over 24 h to P50 + 80 *Fgfr3-iCreER<sup>T2</sup>:R26R-YFP* mice (e) (see Methods). Immunohistochemistry detected many YFP (green), BrdU (red) double-positive cells in the SVZ (single confocal scan; lateral ventricle marked by asterisk). A BrdU<sup>+</sup>, YFP<sup>+</sup> cell (arrow) and a BrdU<sup>+</sup>, YFP-negative cell (arrowhead) are indicated. Scale bars: 40  $\mu$ m (a, e), 300  $\mu$ m (b, c).

To test for stem cell labeling, we generated neurosphere cultures from the SVZ and spinal cords of *Fgfr3-iCreER<sup>T2</sup>:R26R-YFP* mice at increasing times (7–80 days) post-tamoxifen (Fig. 5b,c) and determined the proportion of neurospheres that was YFP<sup>+</sup> in each culture (Fig. 5d). At all times post-tamoxifen, 100% of spinal cord-derived neurospheres were uniformly YFP<sup>+</sup> (Fig. 5d). EZ stem cells are the only cells capable of generating neurospheres in the normal healthy spinal cord, so all adult EZ stem cells must be targeted by the *Fgfr3-iCreER<sup>T2</sup>* transgene. In SVZ cultures, both stem cells (type-B) and progenitor cells (type-C) have the capacity to generate neurospheres (Young et al., 2007). If only the stem cell population expresses *Fgfr3-iCreER<sup>T2</sup>*, then only a fraction of neurospheres should be YFP<sup>+</sup>. However, this fraction would be expected to increase, the longer the delay between tamoxifen administration *in vivo* and establishment of the SVZ cell cultures. This is because YFP<sup>+</sup> stem cells give rise to YFP<sup>+</sup> intermediate progenitor cells, while preexisting (YFP-negative) progenitors generate migratory neuroblasts that leave the SVZ to join the rostral migratory stream (RMS) and

move towards the OB. This is what we found experimentally. Only 31%  $\pm$  11% of neurospheres were YFP<sup>+</sup> in SVZ-derived cultures that were established at the shortest time post-tamoxifen (P70 + 7) (Fig. 5d). However, the proportion of neurospheres that was YFP<sup>+</sup> increased with time post-tamoxifen, to 89%  $\pm$  4% at P70 + 56 and 90%  $\pm$  6% at P70 + 80 (Fig. 5d). These data indicate that ~90% of SVZ stem cells recombine following tamoxifen administration (i.e. recombination efficiency  $\approx$  90%), similar to the recombination rate in fibrous and protoplasmic astrocytes. Consistent with this, BrdU labeling experiments *in vivo* showed that 91%  $\pm$  2% of BrdU<sup>+</sup> cells in the SVZ of adult P50 + 80 *Fgfr3-iCreER<sup>T2</sup>:R26R-YFP* mice were YFP<sup>+</sup> (four BrdU injections in 24 h; Fig. 5e).

If *Fgfr3-iCreER<sup>T2</sup>* is expressed in migratory neuroblasts (type-A cells), one would expect to find YFP-labeling of PSA-NCAM<sup>+</sup> neuroblasts in the SVZ, RMS, and OB at short times post-tamoxifen. Immunolabeling coronal sections of P50 + 7 brains showed that a decreasing proportion of PSA-NCAM<sup>+</sup> neuroblasts was YFP<sup>+</sup> as one moved rostrally from the SVZ to the OB (27%  $\pm$  9% versus 0.4%  $\pm$  0.4%, respectively) (Fig. 6a–c,g). The gradient of recombination (YFP labeling) from SVZ to OB suggests that the *Fgfr3-iCreER<sup>T2</sup>* transgene is not transcribed in PSA-NCAM<sup>+</sup> neuroblasts directly, but that neuroblasts inherit an active YFP reporter from SVZ stem cells, via intermediate progenitors (neither stem cells nor intermediate progenitors express PSA-NCAM). If this is correct, then an increasing proportion of neuroblasts should become YFP-labeled with increasing time post-tamoxifen.

To test this, coronal sections of SVZ, RMS, and OB from P50 + 14, P50 + 80, and P50 + 180 *Fgfr3-iCreER<sup>T2</sup>:R26R-YFP* mice were immuno-labeled for PSA-NCAM and YFP (Fig. 6d–g). At P50 + 14 there was still a rostro-caudal gradient in the proportion of neuroblasts labeled. However, by P50 + 80 the proportion of PSA-NCAM<sup>+</sup> cells that was YFP<sup>+</sup> had reached ~90% in the SVZ, RMS, and OB and this did not increase further, even at P50 + 180 (Fig. 6d–g). These data indicate that the *Fgfr3-iCreER<sup>T2</sup>* transgene is not expressed by migrating neuroblasts but that, with time, they inherit the recombined YFP allele from *Fgfr3<sup>+</sup>* stem cells in the SVZ. Furthermore, since progenitor cells have a limited capacity to generate neuroblasts and must be continually replenished from stem cells, the continued long-term production of YFP<sup>+</sup> neuroblasts (for ~6 months) confirms that the true SVZ stem cell population was labeled in *Fgfr3-iCreER<sup>T2</sup>:R26R-YFP* mice.

### SVZ-Derived Interneurons Accumulate and Survive Long-Term in the Olfactory Bulb

The evidence above demonstrates that *Fgfr3* is expressed by SVZ stem cells (type-B), but not by intermediate progenitors (type-C) or migratory neuroblasts (type-A). Furthermore, we found that no NeuN<sup>+</sup> cells in the OB co-expressed YFP in P50 + 7 *Fgfr3-*

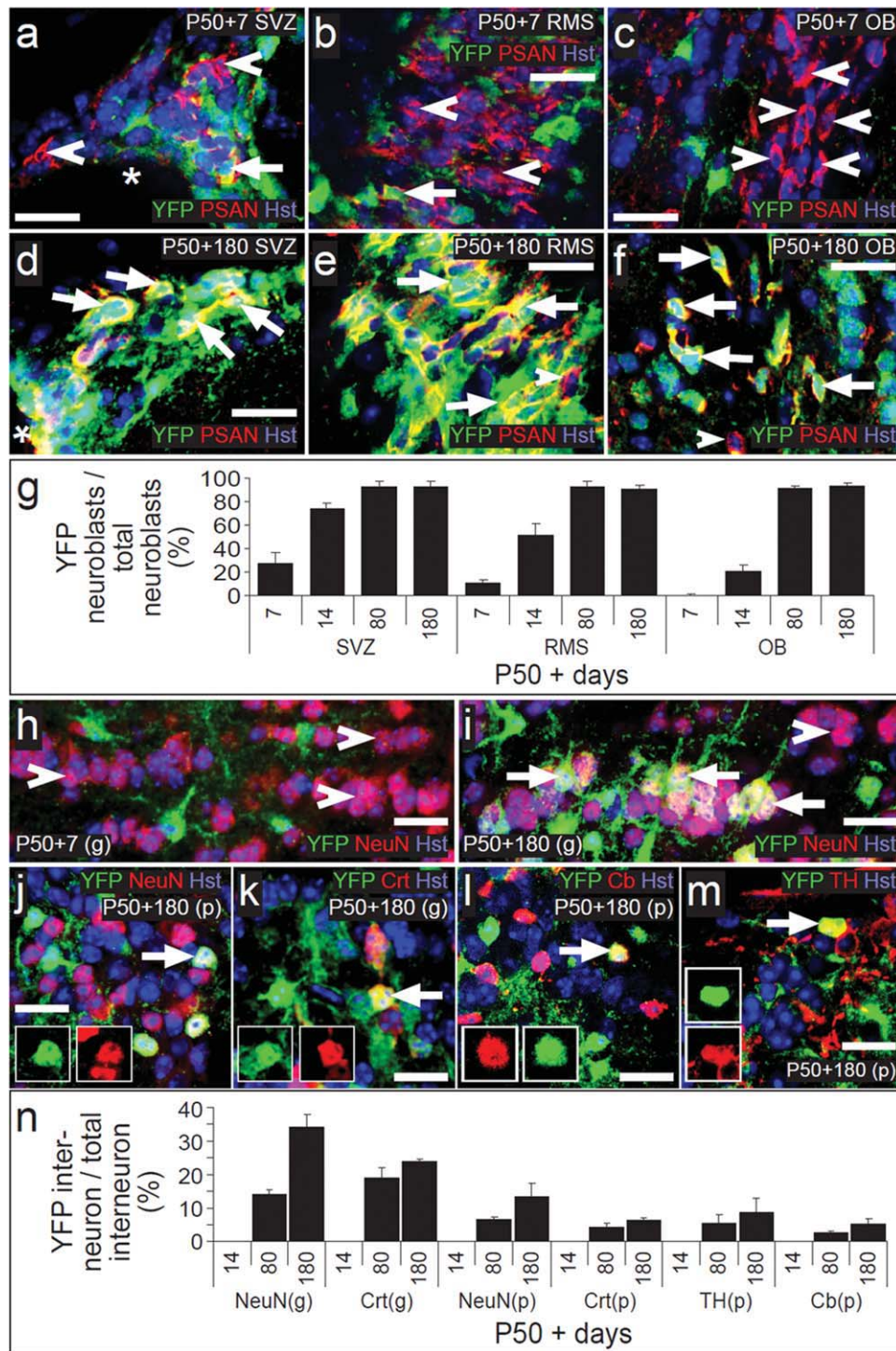


Fig. 6. OB interneurons inherit a recombinant *R26R-YFP* from SVZ stem cells via intermediate PSA-NCAM<sup>+</sup> progenitors. Coronal forebrain sections through the SVZ, RMS and OB of P50 + 7 (a–c), P50 + 14, P50 + 80 and P50 + 180 (d–f) *Fgf3-iCreER<sup>T2</sup>:R26R-YFP* mice were immunolabeled for YFP (green) and PSA-NCAM (red). The proportions of PSA-NCAM<sup>+</sup> cells that were also YFP<sup>+</sup> are shown in (g). At each time point, coronal sections through the OBs of *Fgf3-iCreER<sup>T2</sup>:R26R-YFP* mice were additionally immunolabeled for YFP (green) and either the pan-neuronal marker NeuN (h–j), or the interneuron specific markers calretinin (Crt, k), calbindin (Cb, l), or tyrosine hydroxylase

(TH, m). At each time post-tamoxifen, the proportion of neurons that co-expressed YFP was determined (n). Cell counts were performed across both the granule cell layer (g) and periglomerular layer (p) of the OB. YFP<sup>+</sup> neurons of each subtype accumulated in number up until at least P50 + 180. High magnification single confocal scans (1  $\mu$ m) are shown. Examples of YFP<sup>+</sup> cells are indicated by arrows and YFP-negative cells by arrowheads. Sections were counterstained with Hoechst 33258 (Hst) to visualize cell nuclei. Scale bars: 25  $\mu$ m (a–f), 20  $\mu$ m (h–m).

*iCreER<sup>T2</sup>:R26R-YFP* mice, demonstrating that post-mitotic OB neurons are themselves *Fgfr3*-negative (Fig. 6h). We took advantage of this to investigate the rate of arrival and accumulation of SVZ-derived interneurons in the adult OB. We administered tamoxifen to *Fgfr3-iCreER<sup>T2</sup>:R26R-YFP* mice starting on P50 and analyzed OB sections by immunolabeling for YFP and NeuN 7, 14, 80, or 180 days later (Fig. 6h–j). In addition, we identified interneuron subtypes by immunolabeling for Calretinin, Calbindin, or Tyrosine Hydroxylase (Fig. 6k–m). The proportion of each interneuron subtype that was YFP-labeled increased between P50 + 14 and P50 + 80 and again between P50 + 80 and P50 + 180 (Fig. 6n), as expected if new adult-born neurons arrive in the OB from the RMS and survive in the OB for an extended period of time, at least 6 months. This suggests that the adult-born interneurons integrate into the OB circuitry and fulfil long-term functions in both the periglomerular and granule cell layers.

## DISCUSSION

Finding markers that identify both white and gray matter astrocytes but not other kinds of neural cell in the CNS has been a thorny problem. We showed that *Fgfr3* is expressed by astrocytes in the developing and mature CNS (Pringle et al., 2003) and now we have made an *Fgfr3-iCreER<sup>T2</sup>* PAC transgenic mouse line that can be used with conditional reporters to label astrocytes in the mature CNS. The efficiency of Cre recombination following tamoxifen administration by oral gavage was very high with the *R26R-YFP* reporter; ~90% of all protoplasmic and fibrous astrocytes could be labeled in the adult mouse brain. This is sufficient to allow FACS purification of astrocytes (or other *Fgfr3*<sup>+</sup> cells) for biochemical studies and could also be useful for conditional gene deletion or overexpression. On the *Z/EG* reporter background, recombination was much less efficient, labeling only ~12% of protoplasmic or fibrous astrocytes. Nevertheless, each individual cell was brightly labeled, revealing fine detail of cellular morphology. For some types of experiment (e.g. electrophysiology) this could be a definite advantage.

In general, recombination efficiency depends on both the Cre driver and the Cre-conditional reporter. We have observed with *Fgfr3-iCreER<sup>T2</sup>* and many other Cre lines, both inducible and constitutive, that *R26R-YFP* (Srinivas et al., 2001) consistently gives the highest recombination rates. This presumably reflects structural features of the reporter transgene such as distance between *lox* sites (shorter distances favoring recombination). Strikingly, we observed practically no recombination in adult *R26R-GFP* reporters (Mao et al., 2001), either with *Fgfr3-CreER<sup>T2</sup>* or with other inducible Cre lines such as *Pdgfra-CreER<sup>T2</sup>* (Rivers et al., 2008), although the *R26R-GFP* reporter has many times been used successfully with constitutive Cre lines by ourselves and others. We ascribe the relatively inefficient recombination of *R26R-GFP* to the fact that it contains

three *lox* sites, not two as in *R26R-YFP*. On top of this, *CreER<sup>T2</sup>* is much less active than constitutive Cre, either because of its altered structure or because it is only transiently activated by tamoxifen, or both. The recombination efficiencies of the *R26R-LacZ* and *Z/EG* reporters (Novak et al., 2000; Soriano, 1999) are intermediate between *R26R-YFP* and *R26R-GFP*, with *R26R-LacZ* being rather more efficient than *Z/EG*, although we have not quantified this.

Many markers of mature astrocytes appear to be shared with other glial cell types, particularly radial glia. For example, transgenic lines that express constitutively active Cre under the transcriptional control of human GFAP (hGFAP) or brain lipid binding protein (BLBP) activate recombination in radial glia during embryogenesis and hence label all of their progeny, including neurons and OLs as well as astrocytes (Anthony et al., 2004; Casper and McCarthy, 2006; Hegedus et al., 2007; Malatesta et al., 2003). An *S100β-eGFP* line (Vives et al., 2003) labels embryonic radial glia and both astrocytes and OLs in the postnatal CNS, mimicking endogenous S100β expression. Tamoxifen-inducible *CreER<sup>T2</sup>* lines that are available to label astrocytes include those driven by the human GFAP promoter (*hGFAP*) (Chow et al., 2008; Ganat et al., 2006; Hirrlinger et al., 2006), *GLAST* (Mori et al., 2006; Slezak et al., 2007), or *Connexin 30* (*Cx30*) promoters (Slezak et al., 2007). With the exception of *Cx30-CreER<sup>T2</sup>*, these lines, like our *Fgfr3-iCreER<sup>T2</sup>*, label radial glia and SVZ stem cells as well as astrocytes. This points to a close relatedness between radial glia and astrocytes, presumably connected to the fact that at least some astrocytes develop by direct trans-differentiation from radial glia (i.e. without an intervening cell division) (Hirano and Goldman, 1988; Voigt, 1989).

We also showed that *Fgfr3* is expressed by stem cells in the postnatal SVZ and RMS but not by the progenitor cells or neuroblasts. The latter is consistent with a report that, following a single pulse of BrdU, most BrdU<sup>+</sup> cells in the SVZ (mainly progenitor cells) do not express *Fgfr3* mRNA (Frinchi et al., 2008). It is difficult to label the main population of parenchymal astrocytes without also labeling subependymal astrocytes in the SVZ (the stem cells), as they share several properties, not only with each other but also with embryonic radial glia. Recent gene array studies of parenchymal astrocytes have identified many new genes that are preferentially expressed by astrocytes *in vivo* (Cahoy et al., 2008; Lichter-Konecki et al., 2008; Obayashi et al., 2009); these gene sets could be a rich source of new astrocyte-specific markers in the future.

We have not examined the fates of *Fgfr3*<sup>+</sup> astrocytes following mechanical injury to the CNS. However, in collaborative experiments to be reported elsewhere (WDR and RMJ Franklin, University of Cambridge, UK; manuscript in preparation) we found that, following experimental focal demyelination in *Fgfr3-CreER<sup>T2</sup>:R26R-YFP* spinal cords, YFP<sup>+</sup> reactive astrocytes but no other cell types were generated around the remyelinating lesions. In parallel experiments with *Pdgfra-CreER<sup>T2</sup>:R26R-YFP*

mice, we found few if any YFP-labeled reactive astrocytes. These data suggest that reactive astrocytes are formed from preexisting parenchymal astrocytes and/or EZ stem cells but not from *Pdgfra*-expressing OL precursors/NG2 cells.

We used the fact that our *Fgfr3-iCre<sup>T2</sup>* transgene is expressed in SVZ stem cells to assess their contribution to adult neurogenesis in the OB. There is a variety of interneuron subtypes in the OB. These include the three major populations of GABAergic interneurons in the periglomerular layer, which can be distinguished by immunolabeling for the calcium binding proteins Calbindin and Calretinin and the dopamine synthesizing enzyme tyrosine hydroxylase. The lifespans and functions of these new interneurons has been a matter of great interest in recent years. We report that newly born neurons (YFP<sup>+</sup>, NeuN<sup>+</sup>) accumulate in the periglomerular and granule neuron layers of the OB for at least 6 months after tamoxifen-induced labeling of the SVZ stem cells. By this time, the adult-born interneurons comprise ~15% of all periglomerular interneurons and ~35% of all granule neurons. These data are consistent with a recent study (Imayoshi et al., 2008) in which OB neurogenesis was followed using *Nestin-CreER<sup>T2</sup>* on the *R26R-LacZ* reporter background to label SVZ stem and progenitor cells. These authors demonstrated that adult-born interneurons comprised ~40% of all granule neurons by 6 months post-tamoxifen (Imayoshi et al., 2008). Moreover, it has been established that, in rats, granule neurons that are born at 2 months of age (identified by BrdU pulse-labeling) are still present at 19 months of age (Winner et al., 2002). Our study complements those results by demonstrating that accumulation and long-term survival of adult-born olfactory interneurons is not limited to granule neurons but extends to three distinct sub-classes of periglomerular interneurons.

## ACKNOWLEDGMENTS

We thank Ulla Dennehy and Marta Muller for excellent technical support and our other colleagues in the Wolfson Institute for Biomedical Research (UCL) for helpful comments and discussion. We also thank Yasmin Sabri for contributing to the experiments of Supporting Information Figure 2. KMY is the recipient of an Alzheimer's Society Collaborative Career Development Award in Stem Cell Research. NK was funded by a UK Medical Research Council (MRC) New Investigator Award.

## REFERENCES

- Agius E, Soukkaiech C, Danesin C, Kan P, Takebayashi H, Soula C, Cochard P. 2004. Converse control of oligodendrocyte and astrocyte lineage development by Sonic hedgehog in the chick spinal cord. *Dev Biol* 270:308–321.
- Anthony TE, Klein C, Fishell G, Heintz N. 2004. Radial glia serve as neuronal progenitors in all regions of the central nervous system. *Neuron* 41:881–890.
- Bansal R, Kumar M, Murray K, Morrison RS, Pfeiffer SE. 1996. Regulation of FGF receptors in the oligodendrocyte lineage. *Mol Cell Neurosci* 7:263–275.
- Bansal R, Lakhina V, Remedios R, Tole S. 2003. Expression of FGF receptors 1, 2, 3 in the embryonic and postnatal mouse brain compared with *Pdgfralpha*, *Olig2* and *Plp/dm20*: Implications for oligodendrocyte development. *Dev Neurosci* 25:83–95.
- Bushong EA, Martone ME, Ellisman MH. 2004. Maturation of astrocyte morphology and the establishment of astrocyte domains during postnatal hippocampal development. *Int J Dev Neurosci* 22:73–86.
- Cahoy JD, Emery B, Kaushal A, Foo LC, Zamanian JL, Christopherson KS, Xing Y, Lubischer JL, Krieg PA, Krupenko SA, Thompson WJ, Barres BA. 2008. A transcriptome database for astrocytes, neurons, and oligodendrocytes: A new resource for understanding brain development and function. *J Neurosci* 28:264–278.
- Casper KB, McCarthy KD. 2006. GFAP-positive progenitor cells produce neurons and oligodendrocytes throughout the CNS. *Mol Cell Neurosci* 31:676–684.
- Chow LM, Zhang J, Baker SJ. 2008. Inducible Cre recombinase activity in mouse mature astrocytes and adult neural precursor cells. *Transgenic Res* 17:919–928.
- Claxton S, Kostourou V, Jadeja S, Chambon P, Hodivala-Dilke K, Frutiger M. 2008. Efficient, inducible Cre-recombinase activation in vascular endothelium. *Genesis* 46:74–80.
- Doetsch F, Caille I, Lim DA, Garcia-Verdugo JM, Alvarez-Buylla A. 1999. Subventricular zone astrocytes are neural stem cells in the adult mammalian brain. *Cell* 97:703–716.
- Frinchi M, Bonomo A, Trovato-Salinaro A, Condorelli DF, Fuxe K, Spampinato MG, Mudo G. 2008. Fibroblast growth factor-2 and its receptor expression in proliferating precursor cells of the subventricular zone in the adult rat brain. *Neurosci Lett* 447:20–25.
- Ganat YM, Silbereis J, Cave C, Ngu H, Anderson GM, Ohkubo Y, Ment LR, Vaccarino FM. 2006. Early postnatal astroglial cells produce multilineage precursors and neural stem cells in vivo. *J Neurosci* 26:8609–8621.
- Hachem S, Aguirre A, Vives V, Marks A, Gallo V, Legraverend C. 2005. Spatial and temporal expression of S100B in cells of oligodendrocyte lineage. *Glia* 51:81–97.
- Hamilton LK, Truong MK, Bednarczyk MR, Aumont A, Fernandes KJ. 2009. Cellular organization of the central canal ependymal zone, a niche of latent neural stem cells in the adult mammalian spinal cord. *Neuroscience* 164:1044–1056.
- Hegedus B, Dasgupta B, Shin JE, Emmett RJ, Hart-Mahon EK, Elghazi L, Bernal-Mizrachi E, Gutmann DH. 2007. Neurofibromatosis-1 regulates neuronal and glial cell differentiation from neuroglial progenitors in vivo by both cAMP- and Ras-dependent mechanisms. *Cell Stem Cell* 1:443–457.
- Hirano M, Goldman JE. 1988. Gliogenesis in rat spinal cord: Evidence for origin of astrocytes and oligodendrocytes from radial precursors. *J Neurosci Res* 21:155–167.
- Hirrlinger PG, Scheller A, Braun C, Hirrlinger J, Kirchhoff F. 2006. Temporal control of gene recombination in astrocytes by transgenic expression of the tamoxifen-inducible DNA recombinase variant CreERT2. *Glia* 54:11–20.
- Hochstim C, Deneen B, Lukaszewicz A, Zhou Q, Anderson DJ. 2008. Identification of positionally distinct astrocyte subtypes whose identities are specified by a homeodomain code. *Cell* 133:510–522.
- Imayoshi I, Sakamoto M, Ohtsuka T, Takao K, Miyakawa T, Yamaguchi M, Mori K, Ikeda T, Itoharu S, Kageyama R. 2008. Roles of continuous neurogenesis in the structural and functional integrity of the adult forebrain. *Nat Neurosci* 11:1153–1161.
- Indra AK, Warot X, Brocard J, Bornert JM, Xiao JH, Chambon P, Metzger D. 1999. Temporally-controlled site-specific mutagenesis in the basal layer of the epidermis: Comparison of the recombinase activity of the tamoxifen-inducible Cre-ER(T) and Cre-ER(T2) recombinases. *Nucleic Acids Res* 27:4324–4327.
- Inglis-Broadgate SL, Thomson RE, Pellicano F, Tartaglia MA, Pontikis CC, Cooper JD, Iwata T. 2005. FGFR3 regulates brain size by controlling progenitor cell proliferation and apoptosis during embryonic development. *Dev Biol* 279:73–85.
- Laywell ED, Rakic P, Kukekov VG, Holland EC, Steindler DA. 2000. Identification of a multipotent astrocytic stem cell in the immature and adult mouse brain. *Proc Natl Acad Sci USA* 97:13883–13888.
- Lee EC, Yu D, Martinez DV, Tessarollo L, Swing DA, Court DL, Jenkins NA, Copeland NG. 2001. A highly efficient *Escherichia coli*-based chromosome engineering system adapted for recombinogenic targeting and subcloning of BAC DNA. *Genomics* 73:56–75.
- Lichter-Konecki U, Mangin JM, Gordish-Dressman H, Hoffman EP, Gallo V. 2008. Gene expression profiling of astrocytes from hyperammonemic mice reveals altered pathways for water and potassium homeostasis in vivo. *Glia* 56:365–377.

- Ludwin SK, Kosek JC, Eng LF. 1976. The topographical distribution of S-100 and GFA proteins in the adult rat brain: An immunohistochemical study using horseradish peroxidase-labelled antibodies. *J Comp Neurol* 165:197–207.
- Malatesta P, Hack MA, Hartfuss E, Kettenmann H, Klinkert W, Kirchhoff F, Gotz M. 2003. Neuronal or glial progeny: Regional differences in radial glia fate. *Neuron* 37:751–764.
- Mao X, Fujiwara Y, Chapdelaine A, Yang H, Orkin SH. 2001. Activation of EGFP expression by Cre-mediated excision in a new ROSA26 reporter mouse strain. *Blood* 97:324–326.
- Menn B, Garcia-Verdugo JM, Yaschine C, Gonzalez-Perez O, Rowitch D, Alvarez-Buylla A. 2006. Origin of oligodendrocytes in the subventricular zone of the adult brain. *J Neurosci* 26:7907–7918.
- Miyake A, Hattori Y, Ohta M, Itoh N. 1996. Rat oligodendrocytes and astrocytes preferentially express fibroblast growth factor receptor-2 and -3 mRNAs. *J Neurosci Res* 45:534–541.
- Mori T, Tanaka K, Buffo A, Wurst W, Kuhn R, Gotz M. 2006. Inducible gene deletion in astroglia and radial glia—A valuable tool for functional and lineage analysis. *Glia* 54:21–34.
- Nagy JI, Rash JE. 2003. Astrocyte and oligodendrocyte connexins of the glial syncytium in relation to astrocyte anatomical domains and spatial buffering. *Cell Commun Adhes* 10:401–406.
- Novak A, Guo C, Yang W, Nagy A, Lobe CG. 2000. Z/EG, a double reporter mouse line that expresses enhanced green fluorescent protein upon Cre-mediated excision. *Genesis* 28:147–155.
- Obayashi S, Tabunoki H, Kim SU, Satoh J. 2009. Gene expression profiling of human neural progenitor cells following the serum-induced astrocyte differentiation. *Cell Mol Neurobiol* 29:423–438.
- Oh LY, Denninger A, Colvin JS, Vyas A, Tole S, Ornitz DM, Bansal R. 2003. Fibroblast growth factor receptor 3 signaling regulates the onset of oligodendrocyte terminal differentiation. *J Neurosci* 23:883–894.
- Pringle NP, Yu WP, Howell M, Colvin JS, Ornitz DM, Richardson WD. 2003. *Fgfr3* expression by astrocytes and their precursors: Evidence that astrocytes and oligodendrocytes originate in distinct neuroepithelial domains. *Development* 130:93–102.
- Psachoulia K, Jamen F, Young KM, Richardson WD. Cell cycle dynamics of NG2 cells in the postnatal and ageing mouse brain. *Neuron Glia Biol*, in press.
- Rivers LE, Young KM, Rizzi M, Jamen F, Psachoulia K, Wade A, Kessaris N, Richardson WD. 2008. PDGFRA/NG2 glia generate myelinating oligodendrocytes and piriform projection neurons in adult mice. *Nat Neurosci* 11:1392–1401.
- Shimshak DR, Kim J, Hubner MR, Spengel DJ, Buchholz F, Casanova E, Stewart AF, Seeburg PH, Sprengel R. 2002. Codon-improved Cre recombinase (iCre) expression in the mouse. *Genesis* 32:19–26.
- Slezak M, Goritz C, Niemiec A, Frisen J, Chambon P, Metzger D, Pfrieger FW. 2007. Transgenic mice for conditional gene manipulation in astroglial cells. *Glia* 55:1565–1576.
- Soriano P. 1999. Generalized lacZ expression with the ROSA26 Cre reporter strain. *Nat Genet* 21:70–71.
- Srinivas S, Watanabe T, Lin CS, William CM, Tanabe Y, Jessell TM, Costantini F. 2001. Cre reporter strains produced by targeted insertion of EYFP and ECFP into the ROSA26 locus. *BMC Dev Biol* 1:4.
- Theiler K. 1972. The house mouse: Development and normal stages from fertilization to 4 weeks of age. Berlin: Springer-Verlag.
- Thomson RE, Pellicano F, Iwata T. 2007. Fibroblast growth factor receptor 3 kinase domain mutation increases cortical progenitor proliferation via mitogen-activated protein kinase activation. *J Neurochem* 100:1565–1578.
- Vives V, Alonso G, Solal AC, Joubert D, Legraverend C. 2003. Visualization of S100B-positive neurons and glia in the central nervous system of EGFP transgenic mice. *J Comp Neurol* 457:404–419.
- Voigt T. 1989. Development of glial cells in the cerebral wall of ferrets: Direct tracing of their transformation from radial glia into astrocytes. *J Comp Neurol* 289:74–88.
- Weiss S, Dunne C, Hewson J, Wohl C, Wheatley M, Peterson AC, Reynolds BA. 1996. Multipotent CNS stem cells are present in the adult mammalian spinal cord and ventricular neuroaxis. *J Neurosci* 16:7599–7609.
- Winner B, Cooper-Kuhn CM, Aigner R, Winkler J, Kuhn HG. 2002. Long-term survival and cell death of newly generated neurons in the adult rat olfactory bulb. *Eur J Neurosci* 16:1681–1689.
- Young KM, Fogarty M, Kessaris N, Richardson WD. 2007. Subventricular zone stem cells are heterogeneous with respect to their embryonic origins and neurogenic fates in the adult olfactory bulb. *J Neurosci* 27:8286–8296.
- Zuo Y, Lubischer JL, Kang H, Tian L, Mikesch M, Marks A, Scofield VL, Maika S, Newman C, Krieg P, Thompson WJ. 2004. Fluorescent proteins expressed in mouse transgenic lines mark subsets of glia, neurons, macrophages, and dendritic cells for vital examination. *J Neurosci* 24:10999–11009.